


 Cite this: *RSC Adv.*, 2020, **10**, 34986

# Bio-oils from vacuum ablative pyrolysis of torrefied tobacco residues†

 Nattawut Khuenkaeo,<sup>a</sup> Blake MacQueen,<sup>b</sup> Thossaporn Onsree,<sup>ID</sup><sup>a</sup> Sangu Daiya,<sup>c</sup> Nakorn Tippayawong<sup>ID</sup><sup>\*a</sup> and Jochen Lauterbach<sup>ID</sup><sup>bd</sup>

Fast pyrolysis, in combination with torrefaction pretreatment, was used to convert tobacco residues to value-added bio-fuels and chemicals. Tobacco plant residues were torrefied at 220, 260, and 300 °C, before being pyrolyzed at 450, 500, 550, and 600 °C in a rotating blade ablative reactor under vacuum conditions to test the effects on product yields. With torrefaction, tobacco residues thermally decomposed 20–25% w/w at low temperatures. Torrefaction and pyrolysis temperatures were found to markedly affect pyrolytic product yields of bio-chars and bio-oils, while having no effect on gas-phase products. Bio-oil yields exhibited a direct relation with pyrolysis temperature and an inverse relation with torrefaction temperature. Bio-oils produced were separated into light and heavy oils and analyzed by GC-MS, and <sup>1</sup>H and <sup>13</sup>C NMR. Nicotine was found to be the main compound in the light and heavy oils along with several phenols and cresols in the heavy oil.

 Received 10th July 2020  
 Accepted 25th August 2020

DOI: 10.1039/d0ra06014c

[rsc.li/rsc-advances](http://rsc.li/rsc-advances)

## 1. Introduction

Biomass is considered as a potential alternative resource to reduce the use of fossil fuels due to the fact that it is abundant and renewable, which can be easily found in various forms, such as agricultural residues, wood residues, energy crops, and municipal solid waste, especially from lignocellulosic biomass.<sup>1,2</sup> Besides rice and corn, in Thailand, tobacco is another major economic crop grown<sup>3</sup> which is mainly managed by the Thai tobacco monopoly. During the production process, large amounts of tobacco residues (stalk and leaf fragments) are discarded, and generally, these residues are either heaped on farmland or burnt on-site, leading to a waste of resources and environmental problems, such as air pollution and CO<sub>2</sub> emissions. The conversion of agro-residues to bio-fuels/energy or high-value chemicals presents a solution for the above issues since biomass is identified as a carbon-neutral energy resource.<sup>4</sup> Fast pyrolysis, which is the thermochemical decomposition of organics in the absence of oxygen at rapid heating rates and short hot vapor residence times, offers an ideal pathway to produce fuels and chemicals from various types of biomass.<sup>1</sup> In

general, fast pyrolysis can be used to convert solid biomass residues into liquid-phase products known as bio-oils, which contain many valuable chemicals with yields up to 75% w/w.<sup>5</sup>

In the application of tobacco residues pyrolysis, Lin *et al.*<sup>6</sup> produced bio-chars from slow pyrolysis of tobacco residues. They mentioned that pyrolytic products depended on heating rates and hot vapor residence times. In fast pyrolysis, Chen *et al.*<sup>7</sup> found that bio-oils could be produced with up to 45% w/w yields, which mainly contained nitrogen compounds of alkaloids from nicotine. Without careful management, these alkaloids could be harmful to the environment.<sup>8</sup> Strezov *et al.*<sup>9</sup> exposed the pyrolysis behavior of tobacco residues and showed that there were four-stage mechanisms, which consisted of dehydration, torrefaction, charring, and carbonization. Strezov *et al.*<sup>9</sup> also found that the main chemical compounds of bio-oils by pyrolysis were phenol, acid, and nicotine. Yan *et al.*<sup>10</sup> produced aromatic compounds from bio-oils that were obtained by fast pyrolysis of tobacco leaf and stem at a low temperature of 350 °C. Yan *et al.*<sup>10</sup> also classified the bio-oils into 10 groups of chemical compounds, including heterocycles, acids, alcohols, ketones and aldehydes, amines, phenols, esters, fatty hydrocarbons, saccharides, and others. Furthermore, Liu *et al.*<sup>11</sup> used pyrolysis-gas chromatography-mass spectrometry, thermogravimetric-Fourier transform infrared spectroscopy, and thermogravimetric-mass spectrometry to study characteristic products and mechanism of fast pyrolysis at temperatures between 400 and 800 °C. They showed that the main product compounds were furfural and phenol at low temperatures, while indene and naphthalene at high temperatures.

<sup>a</sup>Department of Mechanical Engineering, Chiang Mai University, Chiang Mai, 50200, Thailand. E-mail: n.tippayawong@yahoo.com; Tel: +66-5394-4146

<sup>b</sup>Department of Chemical Engineering, University of South Carolina, Columbia, 29201, USA

<sup>c</sup>Department of Mechanical Engineering, Nagaoka University of Technology, Niigata, 940-2188, Japan

<sup>d</sup>Center of Economic Excellence for Strategic Approaches to the Generation of Electricity, University of South Carolina, Columbia, 29201, USA

† Electronic supplementary information (ESI) available. See DOI: 10.1039/d0ra06014c



As the heart of a fast pyrolysis process is the reactor, many types of pyrolyzers have been developed, such as bubbling fluid bed, circulating fluid bed, rotating cone, and ablative reactors.<sup>12</sup> Among these reactors, even if an ablative reactor has a limit on scaling up with high costs for industrial process, only this kind of pyrolyzers can be used for large particle sizes of biomass, such as 200 mm.<sup>13</sup> The other pyrolyzers generally require the biomass sizes to be smaller than 10 mm.<sup>14</sup> Biomass in ablative pyrolysis looks like melting butter in a frying pan, where the melting rate depends on pressing the butter down and moving it over the heated pan surface. In an ablative pyrolysis reactor, heat is transferred from the hot reactor surface to the biomass that is mechanically pressed on the hot reactor surface. When the biomass is moved away, the molten layer vaporizes to pyrolytic products. Compared to the other reactors, the reaction rate of ablation is not controlled by heat transfer through the biomass particles,<sup>12</sup> and therefore, larger particles of biomass can be used. In other words, the process in this reactor is limited by the rate of heat supplied to the reactor, rather than the rate of heat absorbed by the pyrolyzed biomass.<sup>12,15</sup> An inert gas to maintain a pyrolytic environment is also not necessary for this type of reactor. However, either a fast flow rate of carrier gas or a vacuum condition in the reactor is needed to remove the pyrolytic products from the reactor in a short hot vapor residence time.

Nowadays, torrefaction and mild pyrolysis of biomass at temperatures between 200 and 300 °C, have become essential pre-treatment steps in biomass thermochemical conversion.<sup>16</sup> Torrefaction slightly changes the bulk density of biomass, and in general, it is combined with a pelleting process to make torrefied biomass pellets.<sup>17</sup> This makes biomass properties more uniform and attractive for process optimization, control, and standardization of the biomass energy production chain.<sup>18</sup> Two-stage biomass pyrolysis, which is torrefaction pre-treatment followed by subsequent fast pyrolysis, is therefore proposed to produce high-quality bio-oils and chemicals.<sup>19</sup> During torrefaction, biomass is dried and, simultaneously, the most reactive components of biomass (mainly hemicelluloses) are thermally decomposed releasing light volatiles rich in oxygen (mostly CO and CO<sub>2</sub>).<sup>20</sup> This results in lower contents of water and acids in pyrolysis bio-oils, leading to higher calorific values.<sup>21</sup> In addition, the combination of torrefaction and fast pyrolysis favors the production of aromatics from biomass.<sup>22,23</sup> To the authors' best knowledge, the application of torrefaction pre-treatment in combination with fast pyrolysis in a vacuum ablative reactor has not yet been reported for tobacco residues. Sun *et al.*<sup>24</sup> recently applied both dry and wet torrefaction at a temperature of 240 °C as a pre-treatment process of tobacco stalk before fast pyrolysis at a temperature of 550 °C in a fixed bed reactor. They suggested that pyrolytic products were improved, especially bio-oils, which contained lower acid contents and higher aromatic hydrocarbons.

Therefore, the objective of the present work is to experimentally investigate the quantity and quality of pyrolytic products, in particular for bio-oils, which were produced by ablative pyrolysis of tobacco residues pre-treated with torrefaction. Tobacco residues were torrefied at 220, 260, and 300 °C for

20 min residence time, and then pyrolyzed at 450, 500, 550, and 600 °C for 10 min residence time in a rotating blade ablative reactor under vacuum conditions. As a reference, the pyrolysis of non-torrefied tobacco residues was also conducted at 600 °C for the same residence time. Yields of the pyrolytic products were presented across all considered conditions. The bio-oils, which were separated into light and heavy oils, were analyzed for their chemical compounds by gas chromatography-mass spectrometry (GC-MS) as well as for functional group determination through <sup>1</sup>H and <sup>13</sup>C nuclear magnetic resonance (NMR).

## 2. Methodology

### 2.1 Tobacco residues sample

Tobacco residues (stalk and leaf fragments) were obtained from the drying and production processes of two tobacco types, Virginia and Burley, which were mixed together uniformly. The residues were manually purified from contaminations on visual inspection; after that, they were grinded and sieved into ~1 cm long particle. The pure tobacco residues were dried in an oven at 105 °C for 72 h and then cooled to room temperature in a controlled-humidity chamber. The dried and pure tobacco residues were stored in zip-lock bags before being used as samples in experiments.

### 2.2 Torrefaction experiments

All samples were torrefied in a fixed-bed flow-through reactor, which was previously used in our research with the same procedure.<sup>17</sup> The torrefaction reaction was enabled *via* the hot gas, ensuring that the flow and the temperature were uniformly distributed across the diameter of the reactor. The heat and mass transfers could occur evenly on the bed everywhere, and all the torrefaction could happen at the same pace. For this work, torrefaction temperatures were varied to set points of 220, 260, and 300 °C, while residence time was fixed at 20 min. High purity research-grade N<sub>2</sub> was used as a carrier gas with a flow rate of 5 L min<sup>-1</sup>. Once the torrefaction experiment was completed, the torrefied tobacco residues were taken out of the reactor and stored in zip-lock bags prior to being subsequently used in vacuum ablative pyrolysis experiments.

### 2.3 Vacuum ablative pyrolysis experiments

The untreated/torrefied tobacco residues were pyrolyzed in a rotating blade ablative reactor under vacuum conditions. The setup of the pyrolysis experiment is shown in Fig. 1, which was adapted from our previous research.<sup>3</sup> The reactor consists in a cylindrical steel tube with an internal diameter of 25 cm and an internal height of 4 cm. In the reactor, the biomass ablation was effectively occurring when four asymmetric blades were rotating and pressing the biomass sample on the surface of the base plate, which was heated to pyrolytic temperatures by a liquefied petroleum gas stove. The general concept of the ablative pyrolysis under atmospheric pressure was discussed in a previous publication.<sup>14</sup> Yet, in the present work, the pressure inside the reactor was reduced by a vacuum pump to establish vacuum conditions for the pyrolytic environment, in which the



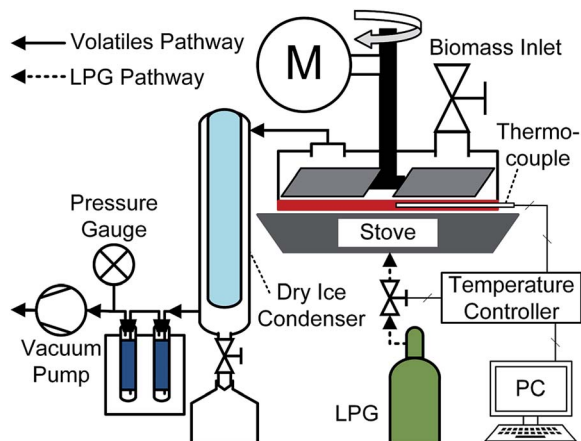


Fig. 1 Setup of vacuum ablative pyrolysis.

inlet pump pressure was maintained at approximately 10.1 kPa. With this approach, during the biomass ablation, volatiles, releasing from the biomass decomposition, could immediately flow out from the reactor, and therefore secondary reactions of the volatiles could not take place. In each test, 50 g ( $\pm 1\%$ ) of the sample was used. Pyrolytic temperatures were varied to set points of 450, 500, 550, and 600 °C for a fixed residence time of 10 min. The rotating blades were set to a speed of 10 rpm. The bio-oils collected were the liquid products condensed in a dry ice condenser during the pyrolysis experiment, while bio-chars were the solid products remaining in the reactor after the experiment was finished. With knowing the mass of both liquid- and solid-phase products, the yield of products was presented across the pyrolysis operating conditions and the torrefaction effects, in which were calculated by eqn (1):

$$y_i = m_i/m_0 \times 100 \quad (1)$$

where  $y$  is the yield of each product, which is represented by a subscript  $i$ , and  $m_0$  is the initial mass of a sample.

#### 2.4 Product analysis

The bio-oil produced from the pyrolysis experimentation was separated *via* separatory funnel into two major sections, light oil and heavy oil. The light and heavy oil samples were analyzed by GC-MS as well as  $^1\text{H}$  and  $^{13}\text{C}$  NMR.

GC-MS was conducted on an Agilent Technologies 7890 GC System coupled with an Agilent 5977B GC/MSD, and a 7693S Autosampler. The system used a DB5-MS column with a length of 30 m, a diameter of 0.25 mm, and a film thickness of 0.50  $\mu\text{L}$ . Prior to analysis, the bio-oil samples were diluted with acetone to ensure that the detector would not saturate. The light oil and heavy oil were diluted to 100 and 310 times their original volume respectively with acetone for analysis. The heavy oil was first diluted by 3.1 times its original volume with acetone to get the heavy oil out of the condenser and was then further diluted by 100 times the solution volume in preparation for analysis. The GC methodology was based on and modified from the procedures described in ref. 25 and 26. 1.0  $\mu\text{L}$  of sample was

injected into the system using a slit ratio of 1 : 10, a column flow of 1 mL  $\text{min}^{-1}$  and a total flow of 14 mL  $\text{min}^{-1}$  using He as the carrier gas, and an injection inlet temperature of 280 °C. The injection needle was cleaned 3 times pre and post injection with 4  $\mu\text{L}$  of acetone. The GC oven was programmed to start at an initial temperature of 40 °C and hold for 4 min followed by a heating ramp of 5 °C  $\text{min}^{-1}$  to 280 °C followed by a 15 min isothermal hold. A solvent cut time of 3 min was utilized before full scan mass spectra were collected scanning from 30–550  $m/z$  with a scan rate of 1562  $\mu\text{s}^{-1}$ , and a scan frequency of 2.8 scans per s. The mass spectrometer source and quadrupole temperature were set to 230 °C and 150 °C respectively. The scans were analyzed using Agilent MassHunter Qualitative Analysis 10.0 and cross-referencing with the NIST17 mass spectral library for component identification. Several Cyclosiloxane compounds were found in the heavy oil spectra and could be attributed to column bleeding of the DB5-MS column.<sup>27</sup> They were manually removed from the spectra for the analysis. Relative area percentages of the product chromatographic peaks were utilized to allow for a semi-quantitative analysis of the bio-oil samples as described in ref. 26.

$^1\text{H}$  and  $^{13}\text{C}$  NMR were conducted on a Bruker 400 Ultra-Shield™ scanning light and heavy oil samples in deuterated acetone. The  $^1\text{H}$  NMR was acquired at 400 MHz and 21 °C, using a 5 mm BBI  $^1\text{H}$ -BB probe resulting in a spectral width of 8278 Hz, and a resolution of 0.126 Hz. The  $^{13}\text{C}$  NMR was acquired at 100 MHz and 22 °C, also using a 5 mm BBI  $^1\text{H}$ -BB probe with a spectral width of 23 980 Hz, and a resolution of 0.366 Hz. The resulting NMR spectra were analyzed in MestReNova and were corrected to the respective acetone reference peaks. The chemical shifts scanned during NMR were 0–16 ppm and 0–220 ppm for  $^1\text{H}$  and  $^{13}\text{C}$ , respectively. The resulting peaks were integrated and then normalized to the total area for analysis and assignment.

## 3. Results and discussion

### 3.1 Torrefied tobacco residues

Fig. 2 shows solid yields of torrefied tobacco residues, in which fluctuations in torrefied tobacco residue yields at any temperatures were assumed to have the same standard error ( $\pm 1.1\%$  w/w), as calculated for the 220 °C condition. The standard error was determined using the standard deviation of the solid yield of three samples at the same torrefaction condition and dividing by the square root of the number of samples. The yields of torrefied tobacco residues were found to lower with higher torrefaction temperatures. But, at 220 and 260 °C, the solid yields appeared not to have a marked change, which was between 80% w/w and 75% w/w, compared to the 300 °C condition, where the yield was slightly above 65% w/w. These numbers were also in similar ranges compared to the literature.<sup>28,29</sup> With torrefaction, thermo-chemical decomposition of agro-residues occurs *via* reactions of dehydration, initial devolatilization, and/or decarboxylation.<sup>30</sup> The three main compounds of lignocellulosic biomass generally respond to this decomposition at different temperature ranges. Hemicellulose is the most sensitive component to the torrefaction process



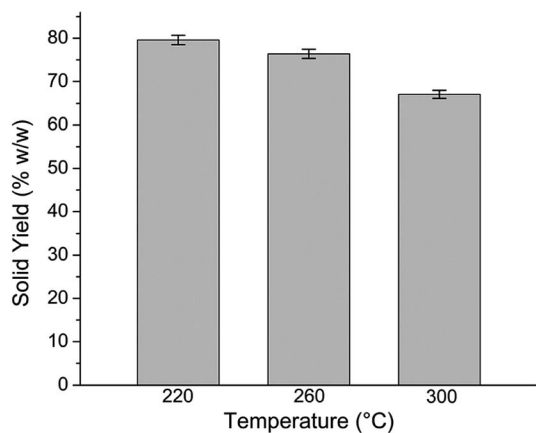


Fig. 2 Solid yields of tobacco residues torrefied at 220, 260, and 300 °C for a fixed residence time of 20 min.

between 220 and 315 °C.<sup>31</sup> Cellulose decomposes within 260–410 °C, while lignin gradually decomposes from 160 to 900 °C.<sup>32</sup> Hence, in this work, tobacco residues thermochemically decomposed between 20–25% w/w at 220 and 260 °C by partial decompositions of hemicellulose and lignin except for cellulose, but about 35% w/w at 300 °C, when the hemicellulose was almost gone and the other components increasingly degraded.

### 3.2 Product yields from pyrolysis

In order to investigate the effect of torrefaction temperatures on the yields of products produced by pyrolysis, tobacco residues were torrefied at 220, 260, and 300 °C for 20 min residence time, prior to being pyrolyzed at 600 °C for 10 min residence time. Similarly, the effect of pyrolysis temperatures was also investigated by subjecting tobacco residues to a fixed torrefaction condition of 220 °C with 20 min residence time for use as samples in the pyrolysis process which tested temperatures of 450, 500, 550, and 600 °C with 10 min residence time. Fig. 3 shows the effects of both torrefaction and pyrolysis temperatures on the yields of bio-char, bio-oil, and gaseous products, compared to those products from pyrolysis of non-torrefied tobacco residues carried out at 600 °C and 10 min. Any changes in product yields at varying torrefaction and pyrolysis

temperatures were approximated to have the same fluctuation as occurred to the pyrolytic condition of untreated tobacco residues, in which they were  $\pm 1\%$  w/w for bio-char yield, and 0.8% w/w for both bio-oil and gas product yields. The standard errors for the bio-char, bio-oil, and gas yields were determined utilizing the standard deviation of three samples at the same conditions and dividing the standard deviation of the yields by the square root of the number of samples. Torrefaction and pyrolysis temperatures were found to have a considerable effect on the pyrolytic product yields of both bio-chars and bio-oils, but not much of an effect on the gas-phase products. Bio-char yields increased from 38% w/w to 50% w/w and bio-oil yields dropped from 48% w/w to 31% w/w when tobacco residues were torrefied at higher temperatures. Compared to the pyrolysis of non-torrefied tobacco residues, the combination of torrefaction and pyrolysis resulted in increased bio-char yields and lowered bio-oil yields. These behaviours were clearer when torrefying temperatures were increased. For example, less than 10% w/w of bio-chars increased at 220 °C condition, but about 20% w/w of those did at 300 °C condition. According to previous pyrolysis studies,<sup>33</sup> bio-chars mostly came from the decomposition of lignin, while bio-oils were mainly from that of hemicellulose and cellulose. When tobacco residues were torrefied at higher temperatures, hemicellulose almost completely decomposed, causing an increase of lignin content in the torrefied biomass, which agreed with previous studies.<sup>34,35</sup> Consequently, in this present work, the yields of both bio-chars and -oils were found to strongly depend on torrefying temperatures, as shown in Fig. 3a. Torrefaction reactions also changed the microstructures of biomass,<sup>36</sup> leading to, during pyrolysis, cross-linking reactions being expedited which resulted in higher bio-char yields and lower bio-oil yields.<sup>37</sup> On the other hand, bio-char yields decreased from 49% w/w to 38% w/w, and bio-oil yields increased from 35% w/w to 46% w/w when pyrolytic temperatures were increased from 450 to 600 °C. These trends were the same, as other pyrolysis works previously found if considering the same range of temperature.<sup>38,39</sup> In addition to increasing conversion of the original lignocellulosic fractions in biomass to pyrolytic products, very high heating and heat transfer rates were achieved at higher pyrolytic temperatures, leading to high pyrolytic reaction rates which minimized bio-char formations

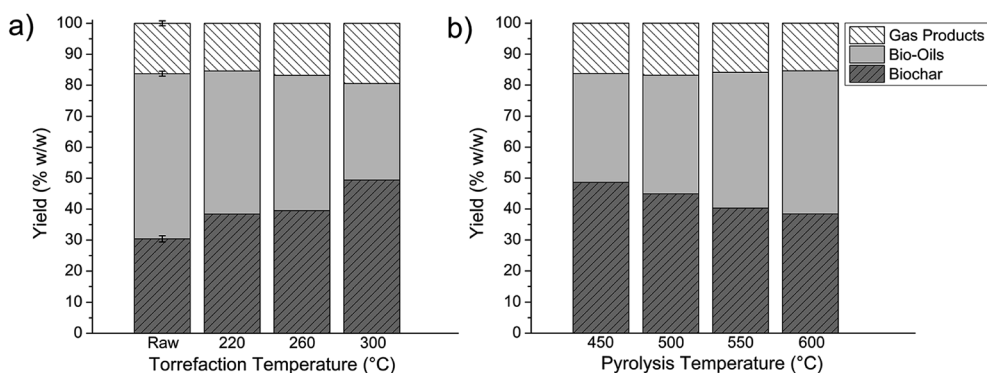


Fig. 3 Yields of pyrolytic char, oil, and gas products from tobacco residues for varying (a) torrefaction and (b) pyrolysis temperatures.

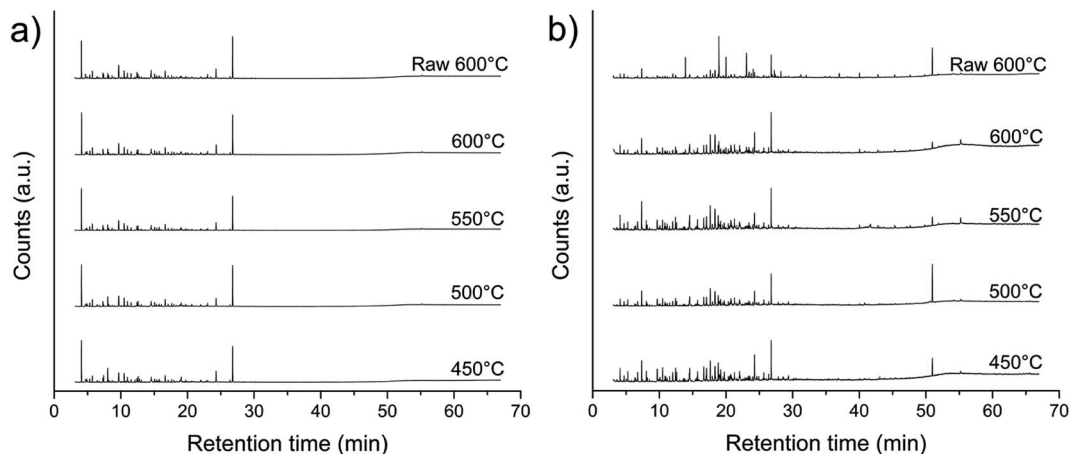


Fig. 4 Normalized GC-MS spectra for bio-oils of torrefied tobacco residues at varying pyrolysis temperatures. (a) light bio-oils (b) heavy bio-oils.

and increased bio-oil yields.<sup>40</sup> In view of the gas-phase products, the yield seemed fairly constant across varying conditions. The gas-phase yield slightly increased from 16% w/w to 20% w/w when torrefaction temperatures were increased from 220 to 300 °C, while maintaining at average of 16% w/w for any cases of increasing pyrolytic temperatures. These insignificant changes in the yield of gas-phase products indicated that secondary reactions, such as vapor cracking, which is due to long vapor residence times within the reactor, did not occur during the pyrolysis process, contrary to another pyrolysis work that previously reported that the yield of gaseous products varied between 13% w/w and 35% w/w over pyrolytic temperatures of 330 to 580 °C.<sup>41</sup> This difference is due to the fact that in a vacuum pyrolyzer, complex organic biomass molecules decompose into primary fragments when being heated, and immediately the fragmented products are vaporized and quickly withdrawn from the reactor to condensers by vacuum; in other words, a very short residence time for volatiles/hot vapor was easily achieved for this type of pyrolysis reactor.<sup>12</sup>

### 3.3 GC-MS analysis

To maximize the bio-oil content while also probing the effect of torrefaction pre-treatment on the product distribution of the bio-oils produced by pyrolysis, light torrefaction conditions of 220 °C and 20 min residence time were utilized for the pre-treatment of tobacco residues before pyrolysis at 450, 500, 550, and 600 °C. The bio-oils produced from the pyrolysis of the torrefied biomass were analyzed in two groups – (i) light and (ii) heavy oils. As a reference, the bio-oils from the pyrolysis of non-torrefied tobacco residues carried out at 600 °C were also analyzed. The light bio-oils were of lower density and were the first products to be condensed in the dry ice condenser which were removed from the condenser without dilution. The heavy bio-oils were of higher density and stuck to the walls of the condenser when being condensed. Therefore, they required dilution with acetone to be extracted. Each pyrolysis experimentation produced roughly 3–5 : 1 volumetric ratio of light to heavy oils. The bio-oils produced were quantified with GC-MS in

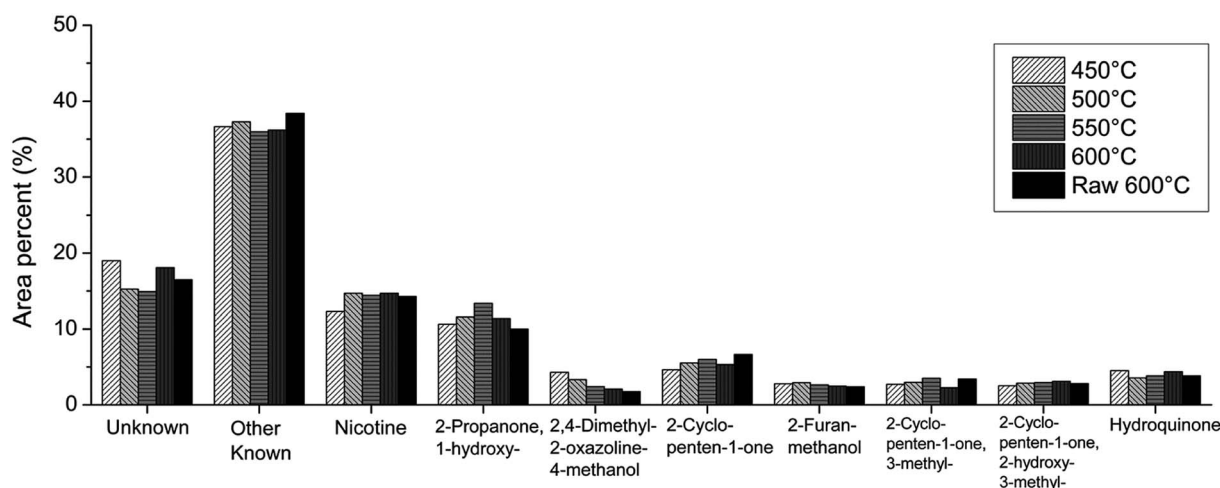


Fig. 5 Main product distribution of light pyrolytic oil of torrefied tobacco residues with varying pyrolysis temperature in terms of GC-MS area percentage. Note: "other known" was from over 50 product compounds each of which had an area% less than a unit.



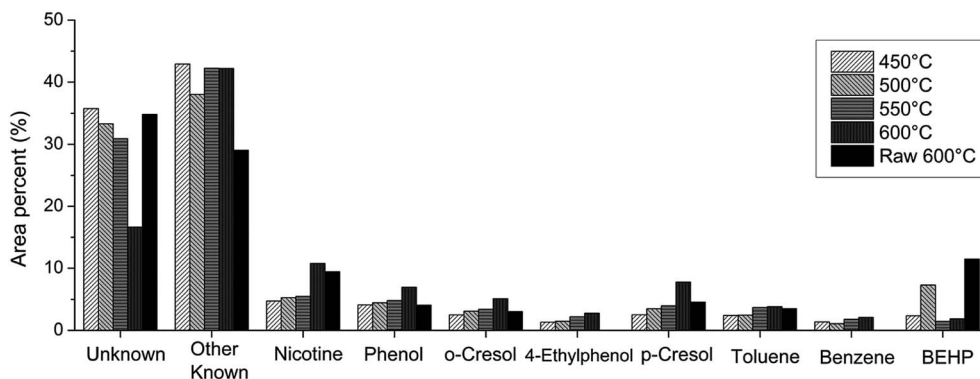


Fig. 6 Main product distribution of heavy pyrolytic bio-oil in terms of GC-MS area percentage. Note "other known" was from over 50 product compounds each of which had an area% less than a unit.

order to determine the products that were produced. The GC-MS spectra for the light and heavy bio-oils are shown in Fig. 4, where the spectra were normalized to the maximum intensity of each respective spectrum.

The main products of the light and heavy bio-oils quantified with GC-MS for different pyrolytic temperatures and torrefaction pre-treatment are shown in Fig. 5 and 6. The full list of products present in the light oils is displayed in Table 1S.† The main products present in the light oils were (*S*)-3-(1-methyl-2-pyrrolidinyl) pyridine, which is also known as nicotine, 1-hydroxy-2-propanone, 2-cyclopenten-1-one, and hydroquinone. Nicotine and 1-hydroxy-2-propanone were the only two products found in over 10 area% of concentration in the GC-MS of the light oils. In the light oils, torrefaction pre-treatment appeared not to have a marked effect on composition of the light oils. For example, the 1-hydroxy-2-propanone concentration was increased from 10.0 area% to 11.4 area% with the utilization of torrefied biomass, while the nicotine concentration was the same within the experimental error between the torrefied and raw light pyrolysis oils. However, a slight change in concentration of the main products was found at the varying pyrolysis temperatures. The nicotine concentrations in the light oil samples were all over 14 area% except for the 450 °C pyrolysis condition, in which it was 12.3 area%. The maximum nicotine concentration was produced at 500 and 600 °C with respective concentrations of 14.7 area%. Based on the literatures, nicotine is considered as a valuable bioactive compound in view of

medical applications.<sup>42,43</sup> The light oil produced by pyrolysis at 550 °C showed a significant increase in 1-hydroxy-2-propanone, and 2-cyclopenten-1-one, which resulted in a slightly lower concentration of nicotine. Only 2,4-dimethyl-2-oxazoline-4-methanol was found to have a significant dependence on the pyrolysis temperature. Here, the concentration of 2,4-dimethyl-2-oxazoline-4-methanol decreased by 48.6% (2.2 area%) from its value measured at the 450 °C pyrolysis when compared with the 600 °C pyrolysis.

For heavy oils, the main products were nicotine, and several phenol and cresol compounds. The full list of products observed in the heavy bio-oils is shown in Table 2S.† Phenols are a common product in lignocellulosic biomass pyrolysis oils<sup>44</sup> and have been utilized in various household products as an antiseptic and are also used as an intermediate for resin and solvent production. Cresols have been found in pyrolysis oils from various sources of lignin<sup>45</sup> and can be used as intermediates to produce materials, such as plastics and pesticides, and assist in the manufacturing of carbon nanotubes. Unlike the light bio-oils, which had little variability and correlation with respect to the pyrolysis temperature, the major heavy bio-oil products showed strong relations with respect to pyrolysis temperature and torrefaction pre-treatment. Most notable were the relation between the nicotine, phenol, and cresols (*o*-cresol and *p*-cresol) with pyrolysis temperature. The concentration of nicotine in the heavy oil increased from 4.74 area% at 450 °C to 5.28, 5.50, and 10.77 area%, respectively, for 500, 550, and

Table 1 <sup>1</sup>H NMR results for bio-oils produced by torrefied biomass pyrolysis (in area%)

Chemical shift region (ppm)	Type of protons	Light oil		Heavy oil	
		450 °C	600 °C	450 °C	600 °C
0.5–1.5	Alkanes	0.84	0.26	2.68	58.69
1.5–3.0	Aliphatic OH, ketones	5.23	0.99	85.55	19.97
3.0–4.4	Alcohols, methylenes	6.35	1.73	11.60	4.92
4.4–6.0	Methoxy, carbohydrates	87.16	96.90	—	2.22
6.0–8.5	(Hetero-) aromatics	0.42	0.12	0.18	14.20
9.5–10.1	Aldehydes	—	—	—	—



600 °C of the pyrolysis reactions. In the heavy oil, the concentration of phenol increased from 4.11 area% at 450 °C to 4.46, 4.82, and 9.92 area%, respectively, for 500, 550, and 600 °C of the pyrolysis reactions. The total concentration of cresols (*o*-cresol and *p*-cresol) increased from 5.03 area% at 450 °C to 6.61, 7.38, and 12.87 area%, respectively, for 500, 550, and 600 °C of the pyrolysis reactions. The largest nicotine concentration (10.77 area%) was achieved by utilizing the 220 °C torrefied biomass followed by a 600 °C pyrolysis. The direct correlation between nicotine, phenol, and cresol concentrations and pyrolysis temperature suggests that these products need more thermal energy to decompose from the biomass. The 220 °C torrefaction pretreatment significantly increased the yield of nicotine, phenol, and cresol compounds in the heavy oil, while the raw biomass that was subjected to the 600 °C pyrolysis had a significantly higher concentration of unknown products. Kibet *et al.*<sup>46</sup> reported that cresols could obtain from the reduction of tyrosine, and the pyrolysis of lignin could provide phenol and cresols. Therefore, torrefied tobacco, which contained higher lignin content, improved the cresol and phenol concentrations in the heavy oils. However, the raw biomass did produce 11.5 area% of bis(2-ethylhexyl) phthalate, which is a commonly used plasticizer, and was only found in a significant concentration in the 500 °C pyrolysis with the pretreated biomass. The concentration of unknown products significantly decreased with increasing pyrolysis temperature, likely due to the reduction in acid compounds, which exhibit an inverse relation with pyrolysis temperature in tobacco pyrolysis oils.<sup>7</sup> However, it is also likely that the unknown compounds also contain amines, phenols and aromatic compounds in addition to the acids, which have been previously reported for tobacco pyrolysis oils.<sup>7</sup> To further investigate the unknown compounds NMR was conducted.

A significant amount of nicotine is present in the tobacco residue biomass as well as potentially valuable products. To maximize the concentration of nicotine produced from the biomass, using a torrefaction temperature of 220 °C followed by a subsequent 600 °C pyrolysis would maximize the total concentration and yield in the combined light and heavy bio-oils. The 600 °C pyrolysis condition also leads to the lowest concentration of unknown products by area percentage in both the light and heavy oils as well as the highest concentration of aromatic products in the heavy oils. The phenols and cresols,

along with the benzene and toluene produced in the heavy oils can be extracted and utilized or sold, further adding to the value to the biomass pyrolysis process. The main drawback of performing the pyrolysis at 600 °C comes down to the added operation cost from using higher operating temperatures. Performing the pyrolysis at 500 °C leads to a slightly lower yield of nicotine but could potentially offset the additional heating costs needed to operate the pyrolysis at 600 °C depending on the scale of the process.

### 3.4 NMR analysis

NMR analysis was conducted on the 450 and 600 °C pyrolysis light and heavy oil samples due to the samples having the most significant differences, and to probe the full effects of pyrolysis temperature. The chemical shift regions as well as the proton and carbon assignments were based on the work previously reported in the literature on pyrolysis oils.<sup>25,47</sup>

The <sup>1</sup>H NMR results and assignments for the various samples are shown in Table 1. There were significant differences in proton concentrations between both light and heavy oils as well as significant effects from pyrolysis temperature. For the light oils, the majority of the protons appeared in the 4.4–6.0 ppm region, which is assigned to methoxy and carbohydrate functional groups. Several of the most abundant compounds in the light oils found in the GC-MS contain methoxy groups. However, the high concentration of protons in this region was not directly expected from the GC-MS results and showed that most likely a large portion of the unknown products contain methoxy and carbohydrate functional groups. For the light oils, less than 1 area% of alkanes was found in the proton NMR. The concentration of aliphatic OH groups and ketones exhibited an inverse relation with pyrolysis temperature, which decreased from 5.23 area% at 450 °C to 0.99 area% at 600 °C. A similar effect was seen for the alcohol and methylene functional group region with the concentration decreasing from 6.35 area% at 450 °C to 1.73 area% at 600 °C. These relations further point to an increase of methoxy and carbohydrate groups being produced in the unknown products at 600 °C pyrolysis, especially since the relative concentration of unknown products is similar between the 450 and 600 °C light oil samples.

For the heavy oils, there was a more significant change in the proton distribution observed in the NMR, which was to be expected based on the GC-MS results and gave further insight into

Table 2 <sup>13</sup>C NMR results for bio-oils produced by torrefied biomass pyrolysis (in area%)

Chemical shift region (ppm)	Type of protons	Light oil		Heavy oil	
		450 °C	600 °C	450 °C	600 °C
0–28	Short aliphatics	25.41	25.46	—	42.05
28–55	Long and branched aliphatics	14.23	12.48	58.30	16.49
55–95	Alcohols, ethers, phenolic-methoxys, carbohydrates	40.66	41.69	—	0.97
95–165	Aromatics, olefins	19.70	17.31	0.99	40.49
165–180	Esters, carboxylic acids	—	1.17	—	—
180–215	Ketones, aldehydes	—	1.88	40.71	—



the unknown products. In the heavy oils, a drastic change in proton concentration was found in the alkane region with the concentration increasing from 2.68 area% at 450 °C to 58.69 area% at 600 °C. This significant increase in the alkane region can be directly contributed to an increase in alkane concentration in the unknown products, or an increase in compounds containing RO–H and RN–H bonds, which can also be found in that region. There was also a significant drop in the aliphatic OH and ketone region from 450 to 600 °C from 85.55 area% to 19.97 area%, respectively. Since a significant portion of products produced in the 450 °C heavy oil contained aliphatic OH or ketone functional groups, these products can be formed from the decomposing biomass at lower temperatures, as compared to nicotine, cresols, and other possible alkane containing products, which form from the torrefied biomass at higher pyrolysis temperatures. The N–CH<sub>3</sub> proton peaks from nicotine<sup>48</sup> and the R–CH<sub>3</sub> peak for cresol<sup>49</sup> are present in the aliphatic OH and ketone region and even with the significant increase in concentration at 600 °C, the total proton area% drastically declines. This shows that a significant portion of the change is resulting from a change in product distribution of the unknown products and the low concentration known products. Acids can have intense chemical shifts in the aliphatic OH and ketone region in <sup>1</sup>H NMR resulting from CH<sub>2</sub> and CH<sub>3</sub> protons.<sup>50</sup> The reduction from 5.23 area% to 0.99 area% in the light oils and 85.55 area% to 19.97 area% for the heavy oils in this region gives further support to the presence of acids in the unknown compounds as previously discussed. Amine compounds can have prominent chemical shifts in the alkane, and aliphatic OH and ketone region in <sup>1</sup>H NMR.<sup>48,51</sup> The significantly higher concentration of protons in the alkane region of the 600 °C heavy oil sample can be partially attributed to an increase in amine concentration, which has been reported to increase significantly with temperature in the 250 °C to 600 °C region.<sup>7</sup> Various amine compounds were seen in the known products of the light oils but were not detected in the known compounds for the heavy oils. The higher concentration of aromatics present in the 600 °C heavy oil sample was consistent with previous work,<sup>52</sup> which has shown that higher pyrolysis temperatures resulted in higher aromatic hydrocarbon yields from biomass. The higher aromatic hydrocarbon yield is further shown by the direct relations seen between the main heavy oil aromatic product (nicotine, toluene, benzene, phenol, and cresol compounds) concentrations and pyrolysis temperature. The significant change in the product concentrations seen in the GC-MS analysis is also reflected in the <sup>1</sup>H NMR results and are complementary to each other, while the NMR also gave further insight into some of the unknown products.

The <sup>13</sup>C NMR results and assignments for the various samples are shown in Table 2. There were more significant changes in the heavy oil samples rather than in the light oil samples for the carbon NMR. For the light oil samples, the carbon distribution was very similar. Most of the carbon was assigned to aliphatics and the alcohol, ester, methoxy, and carbohydrate regions. There were slightly more aromatics and olefins present in the 450 °C sample while the 600 °C sample had slight amounts of esters and carboxylic acids, and ketones

region carbons present. The <sup>13</sup>C NMR shows that there are not significant changes between the respective product distributions produced in the light oil, which is consistent with the GC-MS results.

In the heavy oil, no short aliphatics were found in the oil produced at 450 °C. However, for the 600 °C pyrolysis condition, 42.05 area% of the carbon was assigned to the region containing short aliphatics. There was a higher concentration of long and branched aliphatics in the 450 °C heavy oil than in the 600 °C heavy oil. The total aliphatic carbon concentration was similar between the two heavy oil samples with concentrations of 58.30 area% and 58.54 area% for the 450 and 600 °C samples, respectively. Unlike the proton NMR, only a very small amount of the heavy oil carbons was found to have assignments in the alcohol, methoxy and carboxylic regions for both samples. Rather, there was a significant concentration of ketone and aldehyde assigned carbons in the 450 °C heavy oil, and aromatics and olefins assigned carbons in the 600 °C heavy oil. In the 450 °C heavy oil sample, the carbons in the 180–215 ppm region are representative of ketones due to the exact chemical shifts and the fact that no aldehyde region protons were seen in the <sup>1</sup>H NMR. The higher concentration of aromatic carbons in the 600 °C heavy oil sample further supports the direct relationship between pyrolysis temperature and the concentration of aromatic compounds obtained *via* fast pyrolysis of biomass previously reported in the literature.<sup>52</sup>

## 4. Conclusions

The integration of torrefaction pre-treatment and vacuum ablative pyrolysis can be used to convert tobacco residue biomass to value-added bio-oils, which could be an additional revenue stream to tobacco production. Bio-oil yield showed an inverse relation with torrefaction temperature and a direct relation with pyrolysis temperature. Combining a 220 °C torrefaction pre-treatment with 600 °C fast pyrolysis maximized yields of nicotine and phenol compounds.

## Conflicts of interest

There are no conflicts to declare.

## Acknowledgements

We gratefully acknowledge financial support from the Thailand Research Fund (RSA6180006), Chiang Mai University, the South Carolina Smart State Center for Strategic Approaches to the of Electricity (SAGE), and the National Science Foundation (DGE-1250052).

## References

- 1 R. Kumar, V. Strezov, H. Weldekidan, J. He, S. Singh, T. Kan, *et al.*, Lignocellulose biomass pyrolysis for bio-oil production: A review of biomass pre-treatment methods for production of drop-in fuels, *Renewable Sustainable Energy Rev.*, 2020, **123**, 109763.





- 2 N. Tippayawong, P. Rerkkriangkrai, P. Aggarangsi and A. Pattiya, Characterization of biochar from pyrolysis of corn residues in a semi-continuous carbonizer, *Chemical Engineering Transactions*, 2018, **70**, 1387–1392.
- 3 L. Chumsawat and N. Tippayawong, Utilizing tobacco residues to generate bio-oil and biochar via ablative pyrolysis, *Chemical Engineering Transactions*, 2020, **78**, 49–54.
- 4 Y. V. Fan, C. T. Lee, J. S. Lim, J. J. Klemeš and P. T. K. Le, Cross-disciplinary approaches towards smart, resilient and sustainable circular economy, *J. Cleaner Prod.*, 2019, **232**, 1482–1491.
- 5 A. V. Bridgwater, Renewable fuels and chemicals by thermal processing of biomass, *Chem. Eng. J.*, 2003, **91**(2–3), 87–102.
- 6 Y. Lin, W. Yan and K. Sheng, Effect of pyrolysis conditions on the characteristics of biochar produced from a tobacco stem, *Waste Manage. Res.*, 2016, **34**(8), 793–801.
- 7 H. Chen, G. Lin, Y. Chen, W. Chen and H. Yang, Biomass Pyrolytic Polygeneration of Tobacco Waste: Product Characteristics and Nitrogen Transformation, *Energy and Fuels*, 2016, **30**(3), 1579–1588.
- 8 Z. Chen, M. Wang, E. Jiang, D. Wang, K. Zhang, Y. Ren, *et al.*, Pyrolysis of Torrefied Biomass, *Trends Biotechnol.*, 2018, **36**(12), 1287–1298.
- 9 V. Strezov, E. Popovic, R. V. Filkoski, P. Shah and T. Evans, Assessment of the thermal processing behavior of tobacco waste, *Energy and Fuels*, 2012, **26**(9), 5930–5935.
- 10 B. Yan, S. Zhang, W. Chen and Q. Cai, Pyrolysis of tobacco wastes for bio-oil with aroma compounds, *J. Anal. Appl. Pyrolysis*, 2018, 248–254, DOI: 10.1016/j.jaap.2018.09.016.
- 11 B. Liu, Y. M. Li, S. B. Wu, Y. H. Li, S. S. Deng and Z. L. Xia, Pyrolysis characteristic of tobacco stem studied by Py-GC/MS, TG-FTIR, and TG-MS, *BioResources*, 2013, **8**(1), 220–230.
- 12 A. V. Bridgwater, Review of fast pyrolysis of biomass and product upgrading, *Biomass Bioenergy*, 2012, **38**, 68–94, DOI: 10.1016/j.biombioe.2011.01.048.
- 13 S. Wang, G. Dai, H. Yang and Z. Luo, Lignocellulosic biomass pyrolysis mechanism: A state-of-the-art review, *Prog. Energy Combust. Sci.*, 2017, **62**, 33–86, DOI: 10.1016/j.peccs.2017.05.004.
- 14 N. Khuenkaeo and N. Tippayawong, Production and characterization of bio-oil and biochar from ablative pyrolysis of lignocellulosic biomass residues, *Chem. Eng. Commun.*, 2020, **207**(2), 153–160.
- 15 N. Khuenkaeo and N. Tippayawong, Bio-oil Production from Ablative Pyrolysis of Corn cob Pellets in a Rotating Blade Reactor, *IOP Conference Series: Earth and Environmental Science*, 2018, **159**(1), 012037.
- 16 Y. Chen, H. Yang, Q. Yang, H. Hao, B. Zhu and H. Chen, Torrefaction of agriculture straws and its application on biomass pyrolysis poly-generation, *Bioresour. Technol.*, 2014, **156**, 70–77, DOI: 10.1016/j.biortech.2013.12.088.
- 17 T. Onsree and N. Tippayawong, Torrefaction of Maize Residue Pellets with Dry Flue Gas, *BioEnergy Res.*, 2020, **13**(1), 358–368.
- 18 P. C. a. Bergman, a. R. Boersma, R. W. R. Zwart and J. H. a. Kiel, Torrefaction for biomass co-firing in existing coal-fired power stations, *Energy Res Cent Netherlands ECN ECNC05013*, 2005, July, vol. 71, available from: <http://www.ecn.nl/publications/PdfFetch.aspx?nr=ECN-C-05-013>.
- 19 Z. Chen, E. Leng, Y. Zhang, A. Zheng, Y. Peng, X. Gong, *et al.*, Pyrolysis characteristics of tobacco stem after different solvent leaching treatments, *J. Anal. Appl. Pyrolysis*, 2018, **130**, 249–255, DOI: 10.1016/j.jaap.2017.12.009.
- 20 M. J. Prins, K. J. Ptasiński and F. J. J. G. Janssen, More efficient biomass gasification via torrefaction, *Energy*, 2006, **31**(15), 3458–3470.
- 21 A. Zheng, Z. Zhao, S. Chang, Z. Huang, F. He and H. Li, Effect of torrefaction temperature on product distribution from two-staged pyrolysis of biomass, *Energy and Fuels*, 2012, **26**(5), 2968–2974.
- 22 R. Mahadevan, S. Adhikari, R. Shakya, K. Wang, D. C. Dayton, M. Li, *et al.*, Effect of torrefaction temperature on lignin macromolecule and product distribution from HZSM-5 catalytic pyrolysis, *J. Anal. Appl. Pyrolysis*, 2016, **122**, 95–105.
- 23 S. Neupane, S. Adhikari, Z. Wang, A. J. Ragauskas and Y. Pu, Effect of torrefaction on biomass structure and hydrocarbon production from fast pyrolysis, *Green Chem.*, 2015, **17**(4), 2406–2417.
- 24 Y. Sun, Z. He, R. Tu, Wu Y. jian, J. E. chen and Xu X. wei, The mechanism of wet/dry torrefaction pretreatment on the pyrolysis performance of tobacco stalk, *Bioresour. Technol.*, 2019, **286**, 121390, DOI: 10.1016/j.biortech.2019.121390.
- 25 L. Ingram, D. Mohan, M. Bricka, P. Steele, D. Strobel, D. Crocker, *et al.*, Pyrolysis of wood and bark in an auger reactor: Physical properties and chemical analysis of the produced bio-oils, *Energy and Fuels*, 2008, **22**(1), 614–625.
- 26 B. Onorevoli, M. E. Machado, C. Dariva, E. Franceschi, L. C. Krause, R. A. Jacques, *et al.*, A one-dimensional and comprehensive two-dimensional gas chromatography study of the oil and the bio-oil of the residual cakes from the seeds of *Crambe abyssinica*, *Ind. Crops Prod.*, 2014, **52**, 8–16, DOI: 10.1016/j.indcrop.2013.09.034.
- 27 E. Marco and J. O. Grimalt, A rapid method for the chromatographic analysis of volatile organic compounds in exhaled breath of tobacco cigarette and electronic cigarette smokers, *J. Chromatogr. A*, 2015, **1410**, 51–59, DOI: 10.1016/j.chroma.2015.07.094.
- 28 P. Brachi, R. Chirone, M. Miccio and G. Ruoppolo, Fluidized bed torrefaction of biomass pellets: A comparison between oxidative and inert atmosphere, *Powder Technol.*, 2019, **357**, 97–107, DOI: 10.1016/j.powtec.2019.08.058.
- 29 X. Tian, L. Dai, Y. Wang, Z. Zeng, S. Zhang, L. Jiang, *et al.*, Influence of torrefaction pretreatment on corncobs: A study on fundamental characteristics, thermal behavior, and kinetic, *Bioresour. Technol.*, 2020, **297**, 122490, DOI: 10.1016/j.biortech.2019.122490.
- 30 N. Tippayawong, T. Onsree, T. Williams, K. McCullough, B. MacQueen and J. Lauterbach, Catalytic torrefaction of pelletized agro-residues with Cu/Al<sub>2</sub>O<sub>3</sub> catalysts, *Biomass Convers. Biorefin.*, 2019, DOI: 10.1007/s13399-019-00535-w.
- 31 M. N. Cahyanti, T. R. K. C. Doddapaneni and T. Kikas, Biomass torrefaction: An overview on process parameters, economic and environmental aspects and recent



- advancements, *Bioresour. Technol.*, 2020, **301**, 122737, DOI: 10.1016/j.biortech.2020.122737.
- 32 C. Quan, N. Gao and Q. Song, Pyrolysis of biomass components in a TGA and a fixed-bed reactor: Thermochemical behaviors, kinetics, and product characterization, *J. Anal. Appl. Pyrolysis*, 2016, **121**, 84–92, DOI: 10.1016/j.jaap.2016.07.005.
- 33 Z. Xiong, J. Guo, W. Chaiwat, W. Deng, X. Hu, H. Han, *et al.*, Assessing the chemical composition of heavy components in bio-oils from the pyrolysis of cellulose, hemicellulose and lignin at slow and fast heating rates, *Fuel Process. Technol.*, 2020, **199**, 106299, DOI: 10.1016/j.fuproc.2019.106299.
- 34 B. Ru, S. Wang, G. Dai and L. Zhang, Effect of Torrefaction on Biomass Physicochemical Characteristics and the Resulting Pyrolysis Behavior, *Energy and Fuels*, 2015, **29**(9), 5865–5874.
- 35 S. Wang, B. Ru, G. Dai, H. Lin and L. Zhang, Influence mechanism of torrefaction on softwood pyrolysis based on structural analysis and kinetic modeling, *Int. J. Hydrogen Energy*, 2016, **41**(37), 16428–16435, DOI: 10.1016/j.ijhydene.2016.02.082.
- 36 T. Onsree, N. Tippayawong, T. Williams, K. McCullough, E. Barrow, R. Pogaku, *et al.*, Torrefaction of pelletized corn residues with wet flue gas, *Bioresour. Technol.*, 2019, **285**, 121330, DOI: 10.1016/j.biortech.2019.121330.
- 37 J. Wannapeera, B. Fungtammasan and N. Worasuwanarak, Effects of temperature and holding time during torrefaction on the pyrolysis behaviors of woody biomass, *J. Anal. Appl. Pyrolysis*, 2011, **92**(1), 99–105, DOI: 10.1016/j.jaap.2011.04.010.
- 38 A. Demirbas, Effect of temperature on pyrolysis products from biomass, *Energy Sources, Part A*, 2007, **29**(4), 329–336.
- 39 C. Zhang, Z. Zhang, L. Zhang, Q. Li, C. Li, G. Chen, *et al.*, Evolution of the functionalities and structures of biochar in pyrolysis of poplar in a wide temperature range, *Bioresour. Technol.*, 2020, **304**, 123002, DOI: 10.1016/j.biortech.2020.123002.
- 40 D. Mohan, C. U. Pittman and P. H. Steele, Pyrolysis of wood/biomass for bio-oil: A critical review, *Energy and Fuels*, 2006, **20**(3), 848–889.
- 41 R. J. M. Westerhof, D. W. F. Brilman, W. P. M. Van Swaaij and S. R. A. Kersten, Effect of temperature in fluidized bed fast pyrolysis of biomass: Oil quality assessment in test units, *Ind. Eng. Chem. Res.*, 2010, **49**(3), 1160–1168.
- 42 M. M. Gao, F. Hu, X. Da Zeng, H. L. Tang, H. Zhang, W. Jiang, *et al.*, Hypothalamic proteome changes in response to nicotine and its withdrawal are potentially associated with alteration in body weight, *J. Proteomics*, 2020, **214**, 103633, DOI: 10.1016/j.jprot.2020.103633.
- 43 P. A. Newhouse, Therapeutic applications of nicotinic stimulation: Successes, failures, and future prospects, *Nicotine Tob. Res.*, 2019, **21**(3), 345–348.
- 44 Q. Bu, H. Lei, S. Ren, L. Wang, Q. Zhang, J. Tang, *et al.*, Production of phenols and biofuels by catalytic microwave pyrolysis of lignocellulosic biomass, *Bioresour. Technol.*, 2012, **108**, 274–279, DOI: 10.1016/j.biortech.2011.12.125.
- 45 C. A. Mullen and A. A. Boateng, Catalytic pyrolysis-GC/MS of lignin from several sources, *Fuel Process. Technol.*, 2010, **91**(11), 1446–1458, DOI: 10.1016/j.fuproc.2010.05.022.
- 46 J. K. Kibet, L. Khachatryan and B. Dellinger, Phenols from pyrolysis and co-pyrolysis of tobacco biomass components, *Chemosphere*, 2015, **138**, 259–265, DOI: 10.1016/j.chemosphere.2015.06.003.
- 47 G. D. Strahan, C. A. Mullen and A. A. Boateng, Characterizing biomass fast pyrolysis oils by <sup>13</sup>C NMR and chemometric analysis, *Energy and Fuels*, 2011, **25**(11), 5452–5461.
- 48 M. L. Martin and G. J. Martin, Site-specific isotope effects and origin inference, *Analisis*, 1999, **27**(3), 209–212.
- 49 M. Aiba, X. C. Sun, Y. Shibasaki, M. Oda, C. Ooka, S. Fukuta, *et al.*, Synthesis of poly(o-cresol) by oxidative coupling polymerization of o-cresol, *J. Polym. Sci., Part A: Polym. Chem.*, 2019, **57**(8), 878–884.
- 50 Y. F. Bassuoni, E. S. Elzanfaly, H. M. Essam and H. E.-S. Zaazaa, Development and validation of stability indicating TLC densitometric and spectrophotometric methods for determination of Clobetasol propionate, *Bull. Fac. Pharm.*, 2016, **54**(2), 165–174, DOI: 10.1016/j.bfopcu.2016.05.001.
- 51 N. Kore and P. Pazdera, New stable Cu(I) catalyst supported on weakly acidic polyacrylate resin for green C-N coupling: Synthesis of N-(Pyridin-4-yl)benzene amines and N,N-Bis(pyridine-4-yl)benzene amines, *Molecules*, 2017, **22**(1), 2.
- 52 B. B. Uzun, A. E. Pütün and E. Pütün, Composition of products obtained via fast pyrolysis of olive-oil residue: Effect of pyrolysis temperature, *J. Anal. Appl. Pyrolysis*, 2007, **79**(1–2), 147–153.

